INTERNATIONAL STANDARD

ISO 20958

First edition
2013-08-15

Condition monitoring and diagnostics of machine systems — Electrical signature analysis of three-phase induction motors

Surveillance et diagnostic des systèmes de machines — Analyse de la signature électrique des moteurs triphasés à induction

Reference number
ISO 20958:2013(E)

COPYRIGHT PROTECTED DOCUMENT

ISO copyright office
Case postale 56 • CH-1211 Geneva 20
Tel. + 41 22 749 01 11
Fax + 41 22 749 09 47
E-mail copyright@iso.org
Web www.iso.org

Published in Switzerland

Contents

Page

Foreword

ISO (the International Organization for Standardization) is a worldwide federation of national standards bodies (ISO member bodies). The work of preparing International Standards is normally carried out through ISO technical committees. Each member body interested in a subject for which a technical committee has been established has the right to be represented on that committee. International organizations, governmental and non-governmental, in liaison with ISO, also take part in the work. ISO collaborates closely with the International Electrotechnical Commission (IEC) on all matters of electrotechnical standardization.

The procedures used to develop this document and those intended for its further maintenance are described in the ISO/IEC Directives, Part 1. In particular the different approval criteria needed for the different types of ISO documents should be noted. This document was drafted in accordance with the editorial rules of the ISO/IEC Directives, Part 2, www.iso.org/directives.

Attention is drawn to the possibility that some of the elements of this document may be the subject of patent rights. ISO shall not be held responsible for identifying any or all such patent rights. Details of any patent rights identified during the development of the document will be in the Introduction and/or on the ISO list of patent declarations received, www.iso.org/patents.

Any trade name used in this document is information given for the convenience of users and does not constitute an endorsement.

The committee responsible for this document is ISO/TC 108, *Mechanical vibration, shock and condition monitoring*, Subcommittee SC 5, *Condition monitoring and diagnostics of machine systems*.

Introduction

This International Standard provides guidance for online condition monitoring and diagnostics of machines in the field of electrical signature analysis of three-phase induction motors.

In order to clarify the situation and direct attention towards the latest developments in this field, this International Standard presents an overview of well-established condition monitoring techniques, together with an indication of some which are expected to be less well known.

Condition monitoring and diagnostics of machine systems — Electrical signature analysis of three-phase induction motors

1 Scope

This International Standard sets out guidelines for the online techniques recommended for the purposes of condition monitoring and diagnostics of machines, based on electrical signature analysis. This International Standard is applicable to three-phase induction motors.

2 Normative references

The following documents, in whole or in part, are normatively referenced in this document and are indispensable for its application. For dated references, only the edition cited applies. For undated references, the latest edition of the referenced document (including any amendments) applies.

ISO 13372, *Condition monitoring and diagnostics of machines — Vocabulary*

3 Terms and definitions

For the purposes of this document, the terms and definitions given in ISO 13372 and the following apply.

3.1
current analysis
analysis of the three supply currents to a motor for magnitude, balance, and harmonic content

3.2
current signature analysis
spectral analysis performed on the line current to the motor to determine if there are currents at specific frequencies that can indicate component defects

Note 1 to entry: Traditionally, this has been focused on a single phase, but newer techniques such as Park's vector and voltage and current systems that analyse all three phases simultaneously can provide additional information.

3.3
induction motor
asynchronous AC machine that comprises a magnetic circuit interlinked with two electric circuits or sets of circuits rotating with respect to each other and in which power is transferred from one circuit to another by electromagnetic induction

Note 1 to entry: There are two basic types: squirrel-cage (SCI) and wound-rotor induction motors.

3.4
squirrel-cage induction motor
induction motor in which the secondary circuit consists of usually un-insulated rotor bars in core slots shorted together by end rings connected to both ends of each bar

Note 1 to entry: The most common bar and end ring materials are copper, aluminium, or alloys of these materials.

3.5
wound-rotor motor
induction motor in which the secondary circuit consists of polyphase windings made from insulated multi-turn coils, with each winding phase connected to a slip ring

Note 1 to entry: Control of stator and rotor current during starting and motor torque and speed during running is achieved by connecting external resistances, or a solid-state converter to each rotor winding phase by means of slip rings and brushes.

Note 2 to entry: This type of motor is also known as a slip-ring induction motor.

4 Electrical signature analysis of three-phase induction motors

4.1 General

The vast majority of motors used in industry are induction machines.

Reliability surveys show that the most vulnerable parts of an induction motor are the bearings, the stator winding and core pack, and the rotor cage winding.

There is a lot of published material about a group of monitoring and diagnostic techniques, collectively referred to as electrical signature analysis, that can be used for condition monitoring of induction motors. In general, these techniques are based on the analysis either of signals available at the motor terminals or obtained through appropriate transducers fitted to the structure. Several of these techniques are presented in 4.2 to 4.8.

The purpose of condition monitoring applied to three-phase induction motors is to assess the integrity of the motor and to provide early warning of possible faults. As an aid to this end, it is possible to obtain information about the health and integrity of an induction motor through analysis of its electrical signature. The variations in electric current, voltage, and power can equally be caused by the driven equipment, not just the motor; hence, the requirements of this International Standard, and electrical signature analysis, also apply to assessing the mechanical condition of the driven equipment.

If a motor is supplied from a variable voltage and frequency converter, care must be taken to account for current and voltage components in the output of such devices that could be misdiagnosed as resulting from motor defects. For techniques such as stator current analysis (4.2) and partial discharge (PD) analysis (4.5), it is advisable to lock the converter frequency and voltage while performing these tests.

4.2 Stator current analysis

4.2.1 General

Stator current analysis refers to measurements of the stator current. However, as the stator current is also affected by air gap fluxes and the rotor current, stator current analysis is capable of detecting problems in the rotor and the driven equipment.

4.2.2 Spectral analysis

Current signature analysis (CSA) has the capability of detecting the following problems in squirrel-cage and wound-rotor induction motors, where applicable:

— cracked rotor bars;

— cast rotor windings with large internal voids;

— broken bar-to-short circuit ring connections;

— cracked short circuit rings;

— excessive air gap eccentricity;

— rolling element bearing defects;

— coupling misalignment;

— stator winding shorted turns;

— problems in the driven equipment.

From this list, the most significant and damaging of these are rotor cage winding problems, eccentric air gaps, and rolling element bearing defects. Rolling element bearing defects are included since CSA can identify these defects that may also be identified by vibration monitoring.

Conventional CSA is done online at or close to normal full load. The current on one motor phase is analysed for its current frequency content by measuring it with a clip-on current transformer around a motor supply cable (see Figure 1) or around the secondary side of a current transformer (CT) (see Figure 2). Newer approaches can analyse all three phases and also look at the relation between current and voltage.

Care should be taken when interpreting the results of stator spectral analysis when the motor is driving a time-varying mechanical load since different phenomena can lead to similar characteristic frequencies showing up in the stator current. Some additional means of discriminating between the possible different causes may be required.

4.2.3 Rotor cage defects

CSA monitoring has revolutionized the detection of broken rotor bars and cracked short circuit rings in squirrel-cage induction (SCI) motor rotors. Specific frequencies in the current indicate the presence of defective rotor windings during normal operation of the motor. The detection of broken rotor bars by CSA can sometimes also be confirmed by bearing vibration analysis. References [19] and [27] independently pioneered current signature analysis in the late 1970s.

In simple terms, the current flowing in the stator winding not only depends on the power supply and the impedance of the stator winding, but also includes current induced in the stator winding by the magnetic field from the rotor. That is, the stator winding is a probe or “transducer” for problems in the rotor. The key issue is separating currents that flow through the stator to drive the rotor from the currents that the rotor induces back into the stator if there is a problem. This separation is accomplished by measuring current components at frequencies other than power frequency, using a high-resolution frequency spectrum analyser.

The additional frequency components, due to rotor defects, are seen as sidebands to the fundamental frequency component at frequencies given by Formula (1):

$$f = \left(1 \pm 2ks\right) f_1 \tag{1}$$

where

s is the per unit rotor slip;

f_1 is the fundamental supply frequency;

k is 1, 2, 3, etc.

The rotor currents in a cage winding produce an effective three-phase magnetic field, which has the same number of poles as the stator field, but is rotating at slip frequency with respect to the rotating rotor. If rotor current asymmetry occurs, then there is a resultant backward (i.e. slower) rotating field at slip frequency with respect to the forward rotating rotor. Asymmetry results if one or more of the rotor bars is broken or there are breaks in a short circuit ring preventing current from flowing through them. It can be shown that this backward rotating field is actually rotating forwards at $(1 - 2s)$ times synchronous speed with respect to the stationary stator winding. This induces currents in the stator

winding at a frequency of $f_1(1 - 2s)$, which is referred to as the lower twice slip frequency sideband due to broken bars. This current causes a cyclic variation of current that causes a rotor torque oscillation at twice slip frequency ($2sf_1$) and a corresponding speed oscillation which is a function of drive inertia. This rotor speed oscillation creates an upper side band (Reference [21]) current component at a frequency of $f_1(1 + 2s)$ that is enhanced by the third time harmonic flux. Broken rotor bars, therefore, result in current components being induced in the stator winding at frequencies given by Formula (2):

$$f_{sb} = f_1(1 \pm 2s) \tag{2}$$

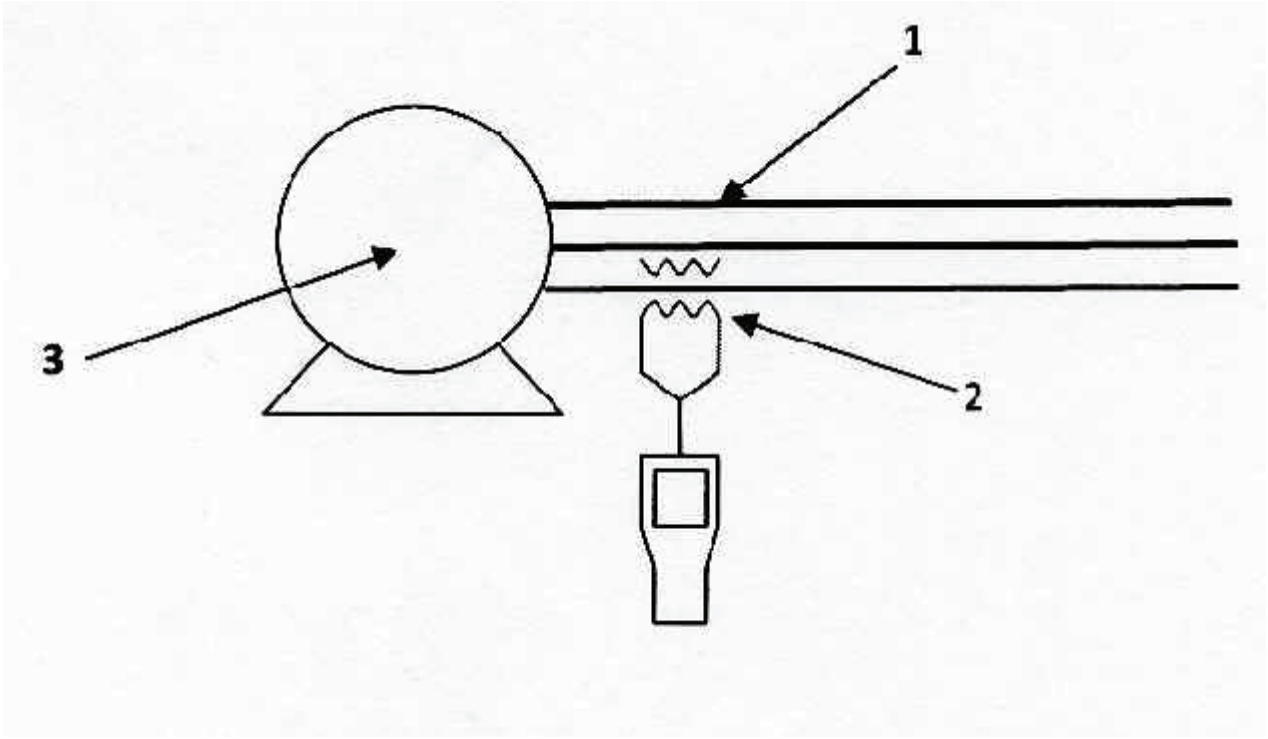

Key

1 phase lead 2 current probe, n_2 3 squirrel-cage induction motor

Figure 1 — Squirrel-cage induction motor CSA measurement on phase lead

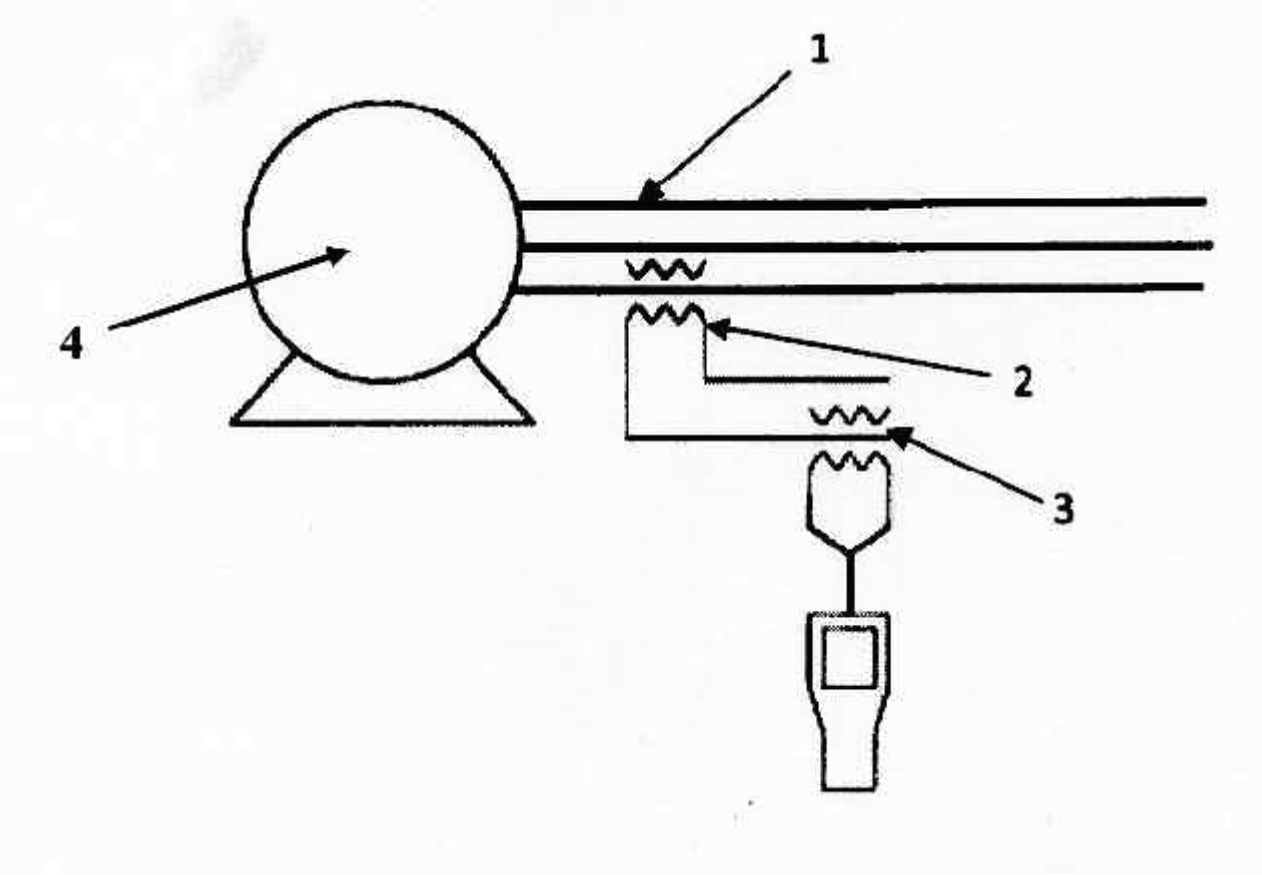

Key

1	phase lead	3	current probe, n_2
2	current probe, n_1	4	squirrel-cage induction motor

Figure 2 — Squirrel-cage induction motor CSA measurement from CT secondary

Current components due to broken rotor bars that appear in a logarithmic amplitude versus frequency plot (such as that shown in Figure 3) as current components that are $\pm 2sf_1$ removed from the fundamental 50 Hz or 60 Hz current component. It is important to note that if the rotor core has the same number of support spider arms as the number of stator winding poles, sidebands with the same frequencies as those from broken bars will result (Reference [16]).

Also, devices such as gearboxes in the motor/driven equipment drive train can create symmetrical sidebands around the fundamental frequency current that can look like those from broken bars. Care should be taken to evaluate sidebands around the fundamental line current that are in the domain of those generated by breaks in rotor cage windings, since there are driven equipment defects that can generate similar patterns. In particular, the various shafts in a gearbox installed between the motor and its driven equipment can produce a series of symmetrical currents around the fundamental line current. The best way to differentiate between such currents and those from cage winding breaks is to perform tests at two significantly different loads to see if there is sideband movement that is proportional to the change in rotor slip.

Because the stator current resulting from breaks in rotor cage winding is modulated at twice the slip frequency, sf_1 is often close to about 1 Hz. This creates a "thrum" sound at this low frequency that is easily recognized by knowledgeable plant staff.

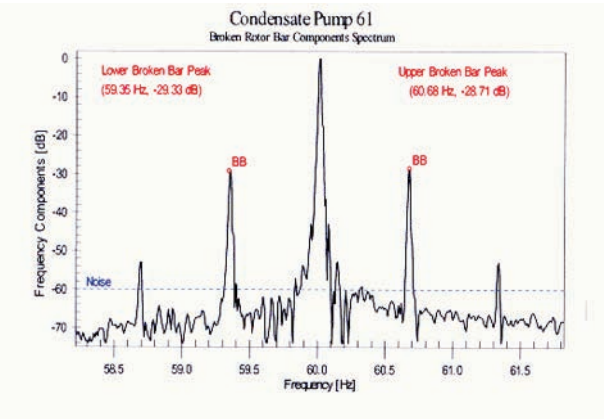

a) 60 Hz motor **b) 50 Hz motor**

Figure 3 — Current signatures of motors with broken bars

The current is analysed with a spectrum analyser or customized digital signal processing unit as shown in Figure 3, which gives examples of both 60 Hz and 50 Hz motors with broken rotor bars. Typically, the sidebands are only 0,3 to 3 Hz or so away from the very large power frequency component and the sideband currents are typically 100 to 1 000 times smaller than the main power frequency currents. The slip "*s*" depends on both the number of poles and slots of the rotor form and the nature of the material constituting the cage winding. The modulation frequency depends not only on the slip rate at rated load, but also the relative I/I_n, where I is the actual current and I_n the motor full load current. Consequently, exceptional dynamic range and frequency resolution is required to accurately measure the sideband peaks due to broken rotor bars. For this reason, current magnitudes are measured in decibels. If there are no rotor cage winding breaks, then there are no or very low-level sidebands.

To detect cage winding breaks, it is necessary that the slip frequency be accurately known. In early "broken rotor bar" detectors, a stroboscope that directly detected the rotor speed (and thus allowed calculation of slip) was used. Alternatively, slip can be detected from an axial flux probe near the rotor winding (Reference[19]). Present-day CSA monitors may have proprietary means of estimating slip from the current itself (Reference[16]). This greatly improves the ease of performing CSA. Some of these methods are effective, but many have been shown to produce errors for small motors, motors that have a large number of poles, or those driving pulsating loads.

Basic interpretation requires comparison of the lower sideband with the power frequency stator current. Experience shows that if the sideband becomes larger than about (≤-50 dB) of the power frequency current, then cage winding breaks are likely. The greater the sideband current (that is, the larger the fraction of the power frequency current), then the more severe the rotor cage winding deterioration. As with most other monitors, it is best to trend the sideband magnitude over the years. If the sideband increases over time at approximately the same load, then it is reasonable to expect that a greater number of bars have broken in more locations. Figures 3 a) and 3 b) show decibel versus frequency plots of motors with several broken bars. At some point, there can be enough breaks in the rotor bars that the motor can fail to start or some metal may fly off the rotor, destroying the stator winding. CSA may not detect bar breaks in large two- or four-pole motors if the breaks occur under endwinding retaining rings since the retaining ring itself can allow the current to continue to flow.

Early CSA monitoring was prone to false indications (that is, indicating that a rotor had problems when it had none) and, less frequently, to missing defective rotor windings. Thus, early users of this test had low confidence in the results. However, improvements in theory, software, and spectrum analyser and

digital signal processor resolution have made detection of rotor cage winding problems much more reliable (Reference [16]).

4.2.4 Air gap eccentricity monitoring

Air gap eccentricity can be detected by identifying the characteristic current signature pattern resulting from abnormal levels of air gap eccentricity. The specific frequencies of the current components indicative of air gap eccentricity may be calculated from Formula (3) (Reference [25]):

$$f_{ec} = f_1\left(R_s \frac{1-s}{p} \pm \eta_{ws}\right) \pm f_1\left(\frac{1-s}{p}\right) \tag{3}$$

where

f_{ec} is the frequency components which are a function of air gap eccentricity (Hz);

f_1 is the supply frequency (Hz);

R_s is the number of rotor slots which is the same as the number of rotor bars;

η_{ws} is 1, 3, 5, etc., [integer 1, corresponds to fundamental component in magneto motive force (m.m.f) waveform, integer 3, 3rd harmonic, etc.];

s is the rotor per unit slip;

p is the pole-pairs.

Formula (3) consists of two parts (Reference [26]): the rotor slot passing frequencies, f_{rs}, as given in Formula (4)

$$f_{rs} = f_1\left(R_s \frac{1-s}{p} \pm \eta_{ws}\right) \tag{4}$$

and the rotor speed frequency, f_r, as given in Formula (5):

$$f_r = f_1\left(\frac{1-s}{p}\right) \tag{5}$$

Thus, air gap eccentricity gives a series of rotor slot passing frequency components with frequencies obtained from Formula (4) with sideband frequencies of $\pm f_r$ obtained from Formula (5).

Experience has shown that the rotor slot passing frequencies can be more easily detected in three-phase induction motors that do not have skewed rotor slots. This is based on the fact that skewed rotor slots reduce the magnitude of the rotor slot passing frequencies flux components and, hence, the electromagnetic forces, resulting in a reduction in stator core vibration and acoustic noise. With an instrument having fast Fourier analysis capability and sufficient resolution, these rotor slot passing frequency components and their sidebands can be detected and their magnitudes measured.

To assess motor air gap eccentricity from this spectrum, the rotor slot passing frequency component (RSPFC) with the highest magnitude is selected. The average magnitude difference between the $\pm f_r$ rotational speed frequency components (RSFC) (in decibels) relative to the RSPFC is then determined (see Figure 4). The lower the average magnitude difference between RSPFC and RSFC, the more eccentric the air gap between the stator and rotor.

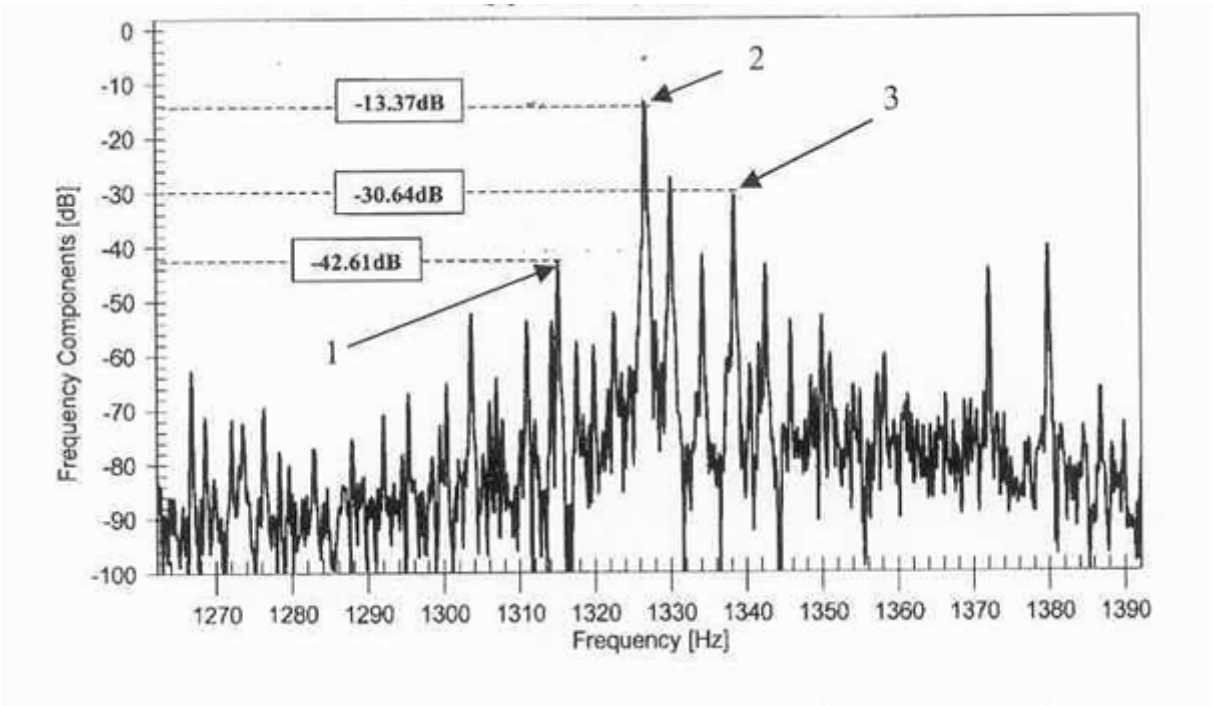

Key

1 RSFC = ($-f_r$) 2 RSPFC 3 RSFC = ($+f_r$)

Figure 4 — Motor with significant air gap eccentricity

4.2.5 Detection of shorted stator winding turns

It has been shown that shorted turns in low-voltage stator windings generate a series of current harmonics that are derived from Formula (6) (ISO 13379[2]):

$$f_{st} = f_1\left[\frac{n}{p}(1-s)\pm k\right] \tag{6}$$

where

f_{st} is the stator winding current components that are a function of shorted turns;

f_1 is the supply frequency (Hz);

η is 1, 2, 3 ...;

k is 1, 3, 5 ...;

p is the pole-pairs;

s is the rotor per unit slip.

4.2.6 Bearing monitoring

Rolling element bearings produce stator current components with a unique set of frequencies for a particular defect. These frequencies are a function of the bearing size and the type and location of a defect. These frequencies can be monitored for defects in the bearing outer race, inner race, and rolling elements. For ball bearings, the formulae given in Table 1 can be used to determine the presence of such defects if the bearing dimensions (see Figure 5) and the number of balls are known (Reference [19]).

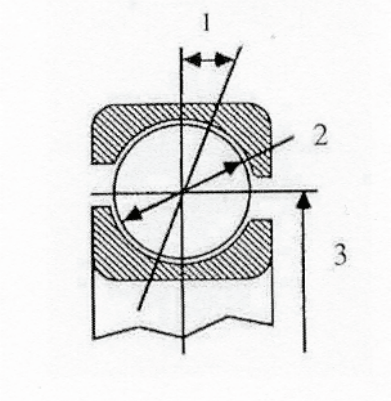

Key

1 contact angle, β 2 ball diameter, D_{ball} 3 pitch diameter, D_{pit}

Figure 5 — Ball bearing dimensions

Table 1 — Bearing defect frequencies

Bearing defect location	Defect frequency
Ball	$f_{rb} = (D_{pit}/D_{ball})f_{rm}\,[1 - (D_{ball}/D_{pit}\cos\beta)^2]$
Outer race	$f_{ro} = (n/2)\,f_{rm}[1 - (D_{ball}/D_{pit}\cos\beta])$
Inner race	$f_{ri} = (n/2)\,f_{rm}[1 + (D_{ball}/D_{pit}\cos\beta)]$

where

f_{rm} is the rotation speed frequency of rotor, equal to revolutions per minute divided by 60;

n is the number of balls;

β is the contact angle;

D_{pit} is the pitch diameter;

D_{ball} is the ball diameter.

The inner and outer race defect frequencies can be approximated from the formulae in Formula (7) if the number of balls is between 6 and 19.

$$f_o = 0,4n\,f_{rm}$$
$$f_i = 0,6n\,f_{rm} \quad (7)$$

The approximate formulae in Formula (7) can also be applied for roller bearings with 12 to 18 rollers.

Therefore, by using an instrument capable of measuring and identifying these current components to see if they are present and dominant, the location of bearing defects can be identified. Also, the magnitudes of current harmonics due to bearing defects can be trended to verify if bearing aging is occurring and a failure may be imminent.

Some CSA instrument software includes details of rolling element bearing dimensions and calculates the expected frequencies for the specific defects given by the formulae in Table 1.

4.2.7 Detection of other mechanical problems

Changes in air gap eccentricity result in changes in the air gap flux waveform. With dynamic eccentricity, the rotor position can vary and any oscillation in the radial air gap length results in variations in the air gap flux. Consequently, this can induce stator current components with frequencies given by Formula (8):

$$f_e = f_1 \pm m f_r \tag{8}$$

where

f_1 is the supply frequency;

f_r is the rotational speed frequency of the rotor;

m is the harmonic number 1,2,3 ...;

f_e is the current component frequency due to air gap changes.

Consequently, problems such as shaft/coupling misalignment, sleeve bearing wear, and other mechanical problems, including some in driven equipment, which result in dynamic rotor disturbances potentially can be detected by looking at the current spectrum.

4.2.8 Park's vector approach

Park's vector is a mathematical approach to represent three phases as two orthogonal phases, which allows for much simpler analysis. This can be used to monitor the induction motor supply currents using the method given in Annex A. This non-invasive approach has been successfully used in industrial environments for diagnosing three-phase induction motor malfunctions such as unbalanced supply voltages, air-gap eccentricity, stator winding inter-turn faults, mechanical misalignment, rotor winding open-circuits in wound-rotor motors, and broken rotor bars or end-rings in cage motors (References [11]–[14]).

An advanced implementation of the Park's vector approach known as the extended Park's vector approach (EPVA) further improves the online fault diagnosis in operating three-phase induction motors (see Annex A). This technique is applicable to motors either directly connected to the main supply or fed from inverters and is also capable of diagnosing three-phase induction motor faults either when they occur singly or in combination.

To differentiate between the effect of rotor faults and the effect associated with driving time-varying loads, the synchronous reference frame Park's vector approach can be used (see Annex A).

4.3 Electrical current, voltage, and power analysis

4.3.1 General

Besides the motor supply current, the supply voltage is also easily accessible and can give some extra information that is necessary to the analysis of the condition of the motor. The electrical power, being a quantity directly related with the current and voltage, acquires particular significance in this context.

Monitoring the three-phase currents, phase-to-phase supply voltages and power input from the motor circuit breaker, or motor control centre (MCC) during running and starting can provide early identification of motor stator- and rotor winding-related defects.

4.3.2 Running tests

Running tests include the following.

— Unbalanced currents due to impedance unbalances, or unbalanced supply voltages: Generally, a small amount of phase voltage unbalance creates a much larger amount of phase current unbalance. The effect of unbalanced voltages on polyphase induction motors is equivalent to the introduction of a "negative sequence voltage" having a rotation opposite to that occurring with balanced phase voltages. This negative phase sequence voltage produces an air gap flux that rotates against the rotation of the rotor, tending to produce higher currents. These currents cause stator and rotor winding overheating if the motor load is not reduced. Unbalanced line currents can also result from phase impedance unbalance due to such defects as high resistance connections or coil turn–turn insulation shorts. The latter are likely to be detected only if the turn insulation short is far removed from the nearest earth.

— Unbalanced supply voltages due to unbalanced loading on the power supply system, or high resistance connections: As indicated above, a small voltage unbalance can create a much larger current unbalance.

— Motor input power monitoring: An increase in motor power consumption with time generally indicates a reduction on the drive system equipment efficiency due to component degradation in either the motor or driven equipment.

— Voltage harmonic analysis: This identifies the presence of harmonics in the motor supply voltage from other devices such as converter-type variable speed motor drives. Such harmonics can be the cause of additional losses in the motor that increase its stator winding operating temperature (Reference [27]).

4.3.3 Starting tests

Starting tests include the following.

— Increases in motor starting time indicate possible breaks in the rotor cage winding and/or increases in driven equipment torque due to component degradation.

— Starting measurements of the first few cycles of current and current until motor rated speed is reached can confirm the presence of high transient current due to a low sub-transient reactance in high-efficiency motors and other causes of motor protection trips.

4.3.4 Model-based voltage and current systems

This is a technique that makes use of the information available from the current and voltage signals across all three phases simultaneously. Model-based systems are able to identify many of the same phenomena also seen by more conventional techniques, covering electrical, mechanical, and operational areas (Reference [17]).

Model-based systems work on the lines shown in Figure 6 below and measure both current and voltage while the motor is in operation and then automatically creates a mathematical model of the relationship between current and voltage. By applying this model to the measured voltage, a modelled current is calculated and this is compared with the actual measured current. Deviations between the measured current and the modelled current represent imperfections in the motor and driven equipment system, which can be analysed using a combination of Park's vector to simplify the three-phase currents into two orthogonal phases (D&Q), Fourier analysis to give a power spectral density plot, and algorithmic assessment of the resulting spectrum to identify specific faults or failure modes.

These systems are designed for permanent installation as a condition monitoring solution rather than as a short-term diagnostic measurement device, and their outputs can be integrated into normal plant systems. Being permanently connected, historic trends are automatically captured.

The sort of output that these types of device can create include single screen, traffic light displays of the overall equipment operation, together with diagnosis of a range of mechanical, electrical, and operational problems, and trend plots showing how these parameters are changing through time. The concept of this type of device is that it can be used by normal plant operators and maintainers without the need for specialist interpretation of spectra, although the underlying spectral plots are available if required.

The sort of faults that can be detected include a range of mechanical problems such as imbalance, misalignment, and bearing problems in the motor and driven equipment, as well as electrical problems including insulation breakdown, loose stator windings, rotor slot problems, current or voltage imbalance, and harmonic distortion. Because these systems measure both current and voltage, they also monitor power and are able to identify problems caused by unusual operating conditions and identify causes of lost efficiency.

Because model-based systems only examine the difference between actual and predicted currents, they effectively filter out all the normal electrical signals that are so apparent in conventional Current Spectral Analysis (CSA), leaving a much simpler set of signals to be analysed.

Because these systems are based on the relationship between voltage and current, they deal well with inverter driven systems where the input voltage may be of a variable frequency and there may be a noisy waveform high in harmonic components. Model-based systems effectively filter out all this noise in the voltage signal from the resulting current signal, leaving just the underlying imperfections.

This ease of use and low cost of this type of equipment makes it appropriate for lower cost, lower criticality equipment.

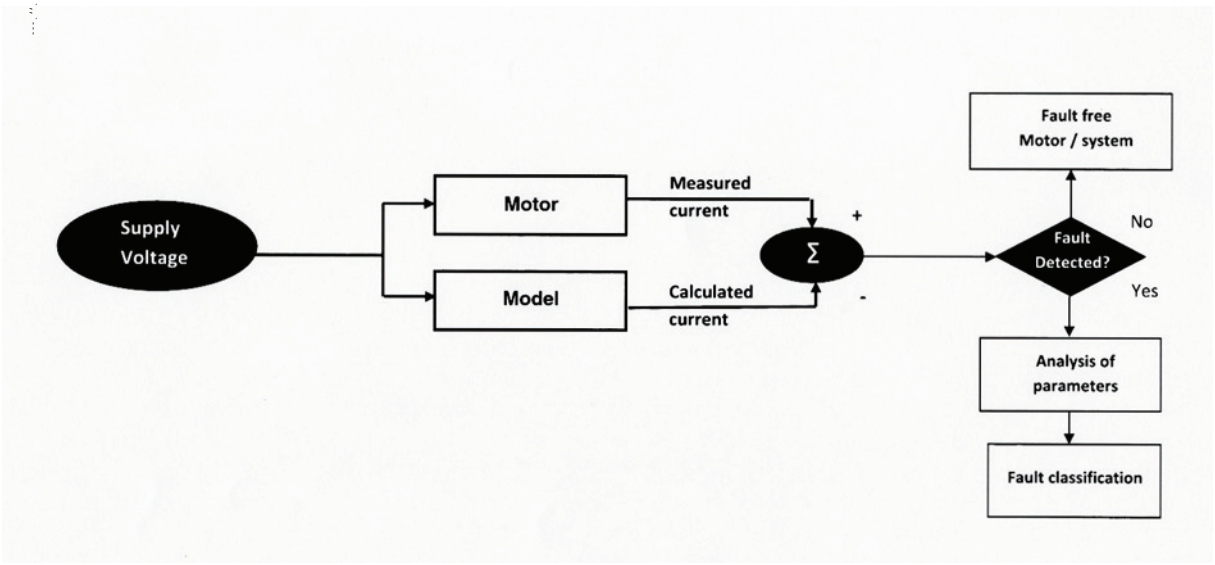

Figure 6 — Model-based voltage and current monitoring system

4.4 Magnetic flux analysis

Any distortion in the air gap flux density due to defects on either rotor or stator sets up an axial homopolar flux in the shaft that can be detected by a search coil fitted around the shaft. A range of both stator and rotor defects can be deduced from the spectrum of the axial flux obtained by carrying out a Fourier transform on the search coil waveform. The technique is applicable to a wide range of motors but there is the possibility that, on some motor designs, the enclosure can attenuate the amplitude of the axial flux detected by a search coil mounted outside it. This makes the quantitative estimate of the extent of damage difficult without fingerprinting of individual motors.

4.5 Partial discharge analysis

4.5.1 Partial discharge principles

Warning of incipient electrical breakdown in a motor stator winding can be obtained by the online measurement of PD activity. Gradual degradation of winding insulation leads to an increase of the PD activity, but a quantitative relationship between that activity and the remaining life of the insulation, which is required for condition monitoring, has not yet been successfully proven.

PDs are small electrical sparks that occur in conventional 50 or 60 Hz stator windings rated 3,3 kV or higher (IEC 60270[6] and Reference [23]). PD is non-existent or negligible in well-made stator windings that are in good condition. However, if the stator winding insulation system is poorly made, or the winding has deteriorated due to overheating, coil movement, or contamination, then PD can occur. A PD test directly measures the pulse currents resulting from PD within a winding. As described in IEEE 1434[7] and IEC/TS 60034-27-2[5] for form-wound stators, there is a large number of test methods. The methods described here are for an in-service motor running at normal load.

PD occurs only when an air-filled void occurs within the stator insulation system or at the surface of the insulation (IEC 60270[6]). At normal atmospheric pressure, when the voltage stress across a void reaches about 3 kV/mm peak and a PD pulse occurs, there is a very fast flow of electrons from one side of the air-filled void to the other side. Since the electrons have charge and are moving close to the speed of light across a small distance, a current pulse results that can have a very short duration, which can be a few nanoseconds. A Fourier transform of a current pulse generates frequencies from DC up to several hundred megahertz (IEEE 1434[7]).

4.5.2 Online PD measurement with capacitive couplers

Any device sensitive to high frequencies can detect the PD pulse currents. In a PD test on complete windings, the most common means of detecting the PD currents on conventional 50 or 60 Hz stators is to use high-voltage capacitors connected to the stator terminal of each phase. Typically for motors, PD couplers with capacitances of 80 pF to 2 nF are connected to the motor terminals as shown in Figure 7 and to a termination box, via coaxial cables, to allow PD measurements. The capacitor is a very high impedance to the high AC voltage in the stator, while being a very low impedance to the high-frequency PD pulse currents. The output of the high-voltage capacitor drives a resistive load. The PD pulse current that passes through the capacitor creates a voltage pulse across the resistor, which can be displayed on an oscilloscope, frequency spectrum analyser, or PD-measuring instrument. The Fourier transform of an individual PD pulse contains frequencies from DC up to several hundred megahertz if the PD sensor is optimally located in close proximity to the PD source. Many types of disturbances produce pulses, but the frequency content of the pulses at the PD sensor can be lower than stator winding PD. For example, sparking caused by poor electrical connections or PD or other PD-like pulses in other apparatus that are remote from the machine under test often produce frequencies up to just a few megahertz. Thus, one method of separating PD from disturbances is to use analogue or digital filters that preferentially respond to pulses in specific frequency ranges. The PD measurement system (sensor and detection electronics) is described as having a lower cutoff frequency and an upper cutoff frequency. Typical frequency ranges for online PD measurement systems are in the low frequency range (LF: below 3MHz), high frequency range (HF: 3MHz to 30 MHz), very high frequency range (VHF: 30 MHz to 300 MHz), or in the ultra-high frequency range (UHF: 300 MHz to 3 GHz) (ISO 13374-1[1]). When using measurement systems in the low frequency range (LF: below 3 MHz) (Reference [18]), the lower frequencies are subject to the significant influence of power line carrier, converter fed motor switching, and excitation system disturbances, which it is necessary to suppress. Elimination of noise that can be assessed as winding PD is an important factor and, to this end, the use of capacitive couplers and long motor power supply cables (≥30 m) has been found to be effective.

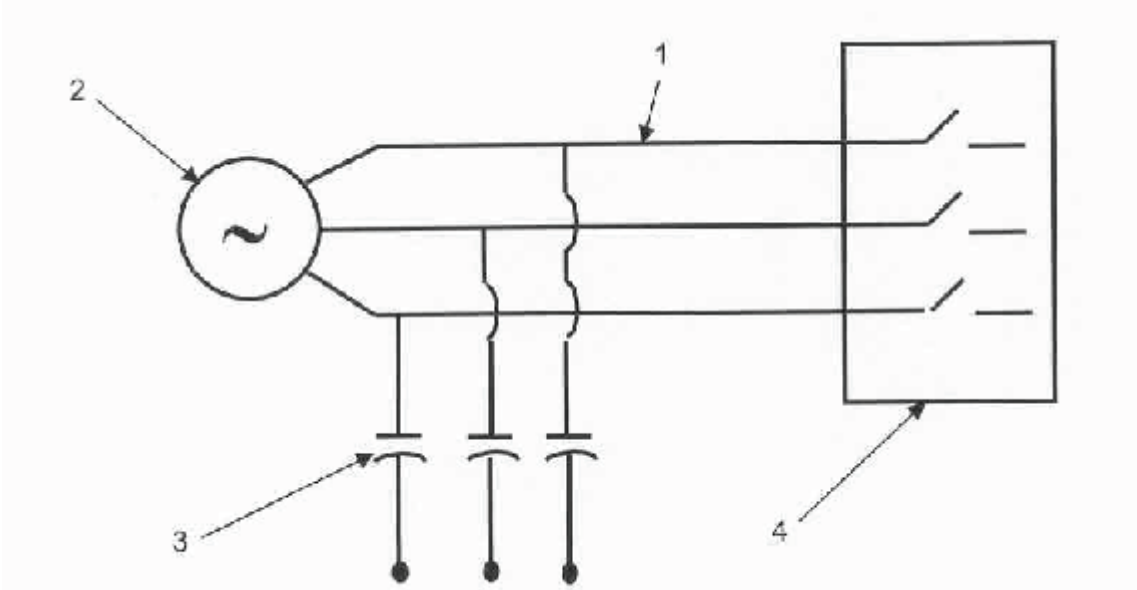

Key

1	power cable	3	PD detection capacitors
2	motor	4	circuit breaker

Figure 7 — Typical arrangement of capacitive couplers for motor PD measurement

Generally, the higher the upper cutoff frequency of the PD detection system, the greater the signal-to-noise ratio, and thus, the lower the risk of false indications. However, the higher the lower cutoff frequency, the lower the likelihood of PD being detected that is remote from the sensor. Assuming the PD sensor is located at the high-voltage terminals of the stator winding, a low-frequency range PD system is sensitive to PD in more coils than a high-frequency range PD system. Note, however, that in online PD testing, the coils near the high-voltage terminal are the only ones likely to have high levels of PD activity since the voltage is higher than that for coils remote from the terminals. However, other sparking and arcing phenomena, which can significantly damage the insulation, can also be detected by PD measurement devices and can occur throughout the winding even at low potential sites close to the neutral, e.g. vibration sparking from coil/bar semiconducting coating material with too low a resistivity. Hence, PD monitoring systems with higher capacitance couplers are more likely to detect insulation degradation from this type of defect.

4.5.3 Online partial discharge monitoring with radio frequency transformers

RF and other high-frequency current transformers can be effective for monitoring motors and any other apparatus that can be prone to PD activity (Reference [17]). These devices are often used because they can be more easily installed and do not operate at high voltage. A current transformer (CT) that has a wideband pulse response can be used to measure high-frequency PD pulses. It is constructed of a ferrite core and is usually encased in a metal housing. Most of the commercially available CTs are provided with a transfer curve describing its frequency response and output signal level. The output signal from a radio frequency transformer (RFCT) may be more oscillatory in nature than from other PD sensors if the CT has not been adequately impedance-matched. In addition, the signal can also contain noise, and the detection of stator winding PD using such devices requires expertise or a sophisticated noise separation technique.

RFCT's coils can be installed around the ground cable to the surge capacitor as shown in Figure 8 (Reference [15]), on cables at motor terminals, on motor grounding conductors, and on connections to ground from cable sheaths. One problem with applying them to surge capacitor ground cables is that there

is significant attenuation of the PD signal, which makes noise separation more difficult. Also, for a single RFCT in a motor grounding (earthing) conductor, the PD from individual phases cannot be identified.

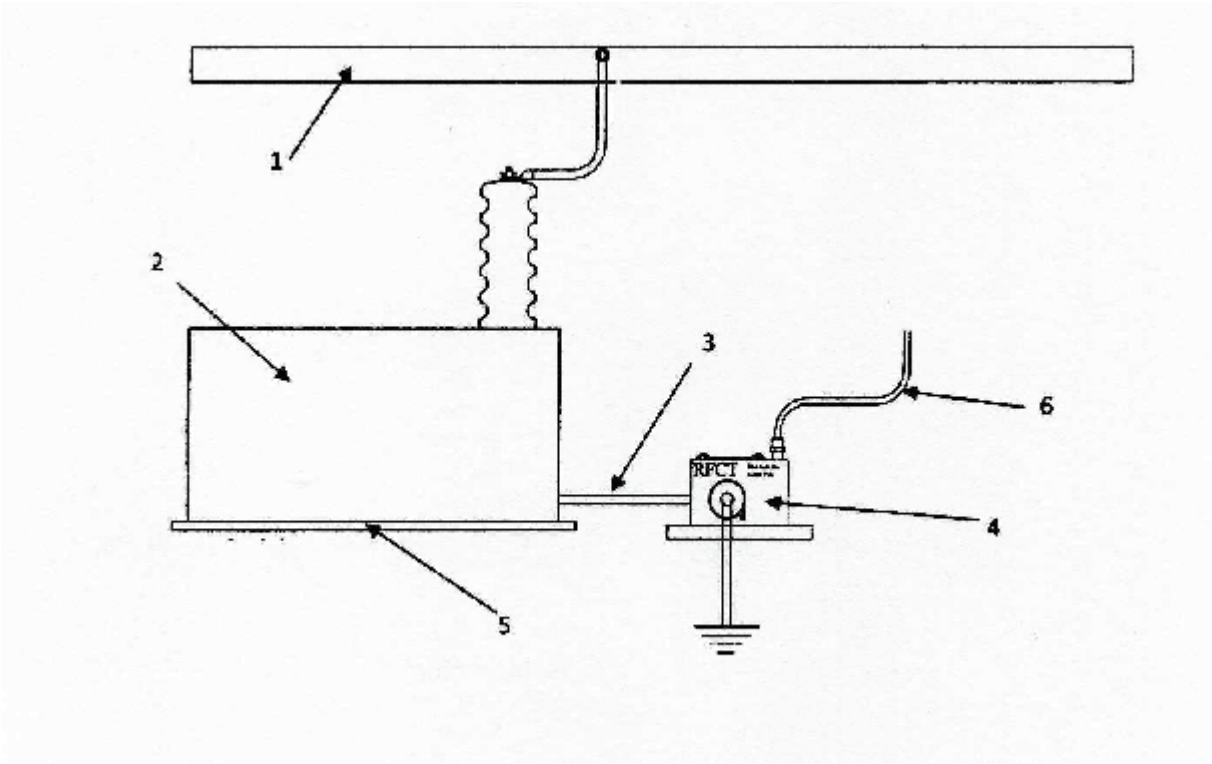

Key

1	bus-to-motor winding	3	surge capacitor grounding cable	5	insulation
2	surge capacitor	4	RFCT	6	coaxial cable for PD measurement

Figure 8 — Partial discharge measurement using RFCT in surge capacitor grounding (earthing) cable

In the case of a CT encircling the primary conductor of a cable, which can be carrying significant 50 Hz or 60 Hz current, there should be an air gap in the magnetic circuit of the CT to prevent saturation.

4.5.4 Insulation defects that partial discharge can detect

Every PD creates its own pulse. Some PD pulses are larger than others. In general, the magnitude of a particular PD pulse is proportional to the size of the void or defect in which the PD occurred. Consequently, the bigger the detected PD pulse, the larger the defect that originated the discharge. In contrast, smaller defects tend to produce smaller PD pulses. The attraction of the PD test is that one concentrates on the larger pulses and ignores the smaller pulses. The PD test enables the measurement of what the biggest defects are. Since failure is likely to originate at the biggest defects and not at the smaller defects, the PD test can indicate the condition of the winding at the portion showing maximum deterioration.

The key measurement in a PD test is the peak PD magnitude, Q_m, i.e. the magnitude of the highest PD pulse. Generally, this value is determined for a specific pulse repetition rate. Figure 9 gives an example for a pulse repetition rate of 10 pulses per second (PPS). Note that Q_m may be measured in terms of mV, pC, mA, or μV.

There is no standard for the PD detector time constant; operating bandwidth or other characteristics of the PD measuring systems are provided by the various suppliers so comparison of data from different PD measuring systems is therefore difficult. However, PD tests can be compared if the results are obtained using the same equipment (PD couplers and instrument) and a value analysis method of Q_m is available. One can determine which phase has the highest Q_m, and, thus, which phase has the greatest

deterioration. One can also compare several similar machines to see which has the highest PD. Finally, one can compare the PD from the same stator over time, i.e. trend the data. In general, if the PD doubles every six months, then the rate of deterioration is increasing rapidly.

Analysis of PD test data to determine its characteristics allows identification of winding insulation degradation and manufacturing defects. Table 2 summarizes the common stator winding insulation deficiencies that manufacturers of PD monitoring equipment claim to be able to identify from the location of PD pulses relative to one cycle of motor phase-to-ground voltage.

Examples of PD pulse patterns from both high- and low-frequency PD measurement systems and for both mV and pC units are given in Figures 10 to 12. As can be seen from Figures 10 and 11, there are patterns approximately centred on 45° and 225° in the phase-to-ground voltage cycle that have similar pulse magnitudes in the positive and negative half cycles of voltage indicating stator winding groundwall insulation delamination from bonding resin thermal aging. Figure 10 shows the phase angle, Φ, at which the PD occurs, plotted against the magnitude, q, of each individual discharge. The number of discharges occurring at each point is shown by the colour, ranging from green indicating low density or individual pulses, through yellow to red for higher concentrations of discharges. Figure 11 plots the pulse magnitude against phase angle of occurrence with a colour code to indicate magnitudes of PD pulses for different ranges of pulse per second (PPS) repetition rates. Figure 12 shows pulse patterns in two phases that are in-phase, opposite polarity and centred on angles that are ± 30° from the "classic" 45° and 225° phase angles, which meets the criteria for interphasal PD.

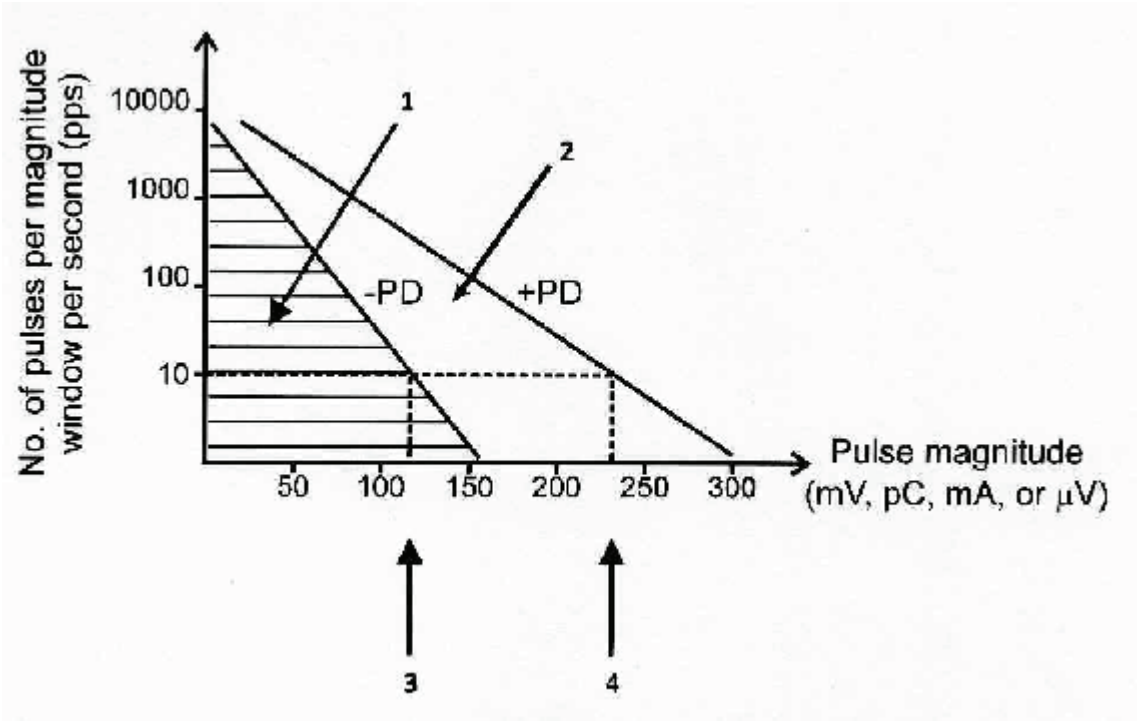

Key

1 −NQN: proportional to the area under voltage negative half cycle PD plot

2 +NQN: proportional to the area under voltage positive half cycle PD plot

3 $-Q_m$: negative PD pulse magnitude at 10 pulses per second

4 $+Q_m$: positive half cycle PD magnitude at 10 pulses per second

Figure 9 — PD summary values

Table 2 — Insulation deficiencies detectable by PD monitoring

Insulation deficiency	Location of PD pulses relative to phase-to-ground voltage	Other factors affecting PD levels	Comments
Groundwall insulation thermal degradation	Clumps of negative PD around 45° and positive PD around 225° of approximately equal magnitudes (see Figure 11)	Winding temperature: the higher the temperature the lower the PD magnitudes	This type of degradation causes delamination of the groundwall insulation due to thermal aging of the bonding resin. The resulting void distribution if fairly uniform throughout the thickness of the groundwall insulation. Can also be detected by off-line test
Thermal cycling	Clumps of negative PD around 45° and positive PD around 225°, with negative PD significantly higher than positive PD	Levels can also decrease with winding temperature increase	Groundwall insulation starts to separate from the conductor stack due to shear stress created by differences in coefficients of expansion of copper and insulation, i.e. that of copper is much higher. More likely to occur in large motors with long cores. Voids next to the conductors can also result from poor resin penetration in vacuum pressure impregnated (VPI) windings. Can also be detected by off-line test
Windings loose in slots	Clumps of negative PD around 45° and positive PD around 225°, with positive PD significantly higher than negative PD	Magnitude of positive PD increases with motor load	Positive PD magnitudes affected by magnitude of current I passing through the stator winding. Resulting 100 or 120 Hz electromagnetic forces proportional to I^2. Positive PD levels can often be reduced by re-wedging. Not a common problem with global VPI windings. Cannot be detected by off-line test
Degraded conductive slot voltage stress control coating	Clumps of negative PD around 45° and positive PD around 225°, with positive PD significantly higher than negative PD	Magnitude of positive PD does not increase with motor load	Painted coatings are more susceptible to degradation than tape types. Can also be detected by off-line test
Degraded voltage grading to conductive coating interfaces coating located outside stator slots	Clumps of PD at zero voltage crossings of 0° and 180° and at 90° and 270° if serious degradation	This occurs on coils near the line end of each phase where the voltage stresses across the interface are highest	This is a very slow insulation degradation mechanism since the PD is acting parallel to the insulation surfaces. Can be detected by ultraviolet camera from an off-line test
Inadequate spacing and/or contamination of endwindings, interphasal connections, or terminal box connections	Clumps of PD displaced from 45° and 225° positions by ± 30° in different phases, that is in-phase and of opposite polarity (see Figure 12)	Levels of PD activity vary with air humidity. An increase in air humidity generally decreases PD levels	PD due to contamination can be reduced by winding cleaning and that due to inadequate spacing, by filling spaces between phases with an insulating material such as electrical grade silicone rubber. May be detected by off-line test

It should be noted that PD monitoring cannot detect the following stator winding aging mechanisms:

— loose endwinding bracing that can lead to insulation degradation from abrasion due to relative movement between components;

— degradation of coil turn insulation from thermal aging, abrasion from loss of bond between strands/conductors, which causes weakening of the turn insulation that can result from failure when winding is exposed to high-magnitude voltage surges.

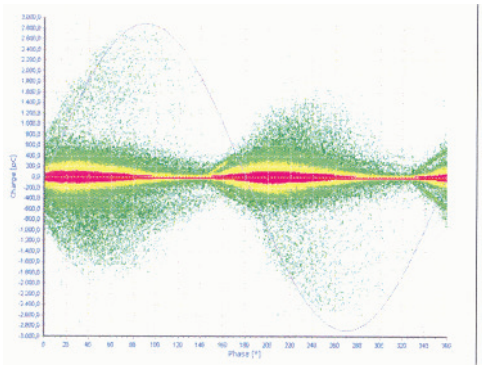

Figure 10 — Low-frequency *Φ-q-n* graph for stator winding phase with thermal aging
(Reference [18])

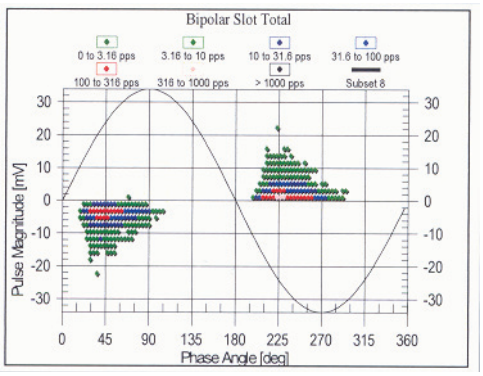

Figure 11 — High-frequency pulse phases analysis plot for stator winding phase with thermal aging

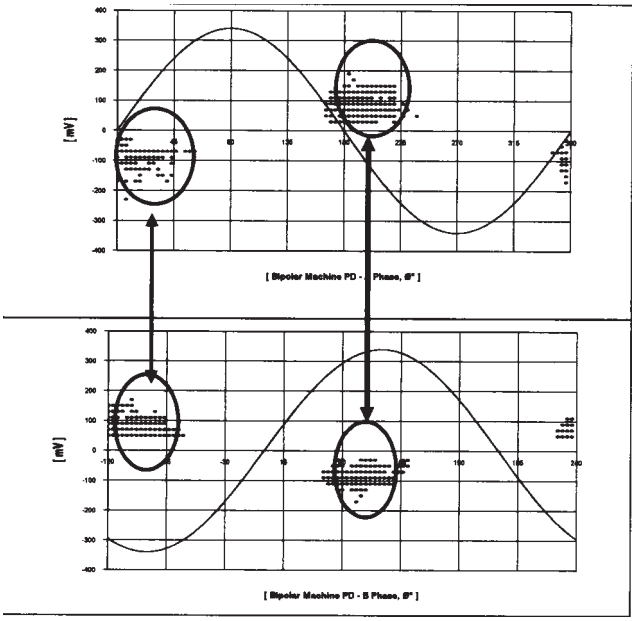

Figure 12 — Interphasal PD due to contamination or inadequate spacing

4.6 Electromagnetic interference testing

Electromagnetic interference (EMI) testing is a technique that can detect and identify partial discharge (PD) activity resulting from insulation defects as well as arcing conditions that result from conductor

and mechanical defects. EMI has been applied to induction motors at utility, petrochemical, and heavy industrial applications. The test is performed while the motor is in service during normal load conditions. EMI is the precise frequency domain measurement and identification of radio frequency energy that results from electrical PDs, discussed in 4.5.3, and arcing at motor defects such as shaft currents through a bearing rub or a seal rub, broken rotor bars, broken stator conductors, loose connections, inadequate shaft grounding, and some types of mechanical problems such as coupling misalignment.

EMI testing follows CISPR 16-1-1[8] and does not require installation of any permanent hardware. It also does not introduce any signals and will not cause any equipment to trip off-line. It utilizes a split-ring radio frequency current transformer (RFCT) that is placed around the safety ground or power conduit of the motor being tested and measures the signals generated from the component or system defects.

EMI diagnostics measure a broad spectrum of radio frequencies to allow the EMI engineer to view various patterns at each frequency, including, but not limited to, corona, gap discharges, random noise, and arcing. Generally, such spectrums display signal magnitude in microvolts (quasi-peak) against frequency, as shown in Figure 13. Corona discharge, gap discharge, and random noise are types of PD each with a unique pattern. The fourth pattern, arcing, may not be measured by PD techniques, since it has a current flow and by definition is not a PD. A handheld instrument can be utilized in conjunction with the EMI software to further identify and pinpoint each defect location. This device measures the EMI signals radiated from each component or system defect and allows an EMI engineer to listen to the radio noise generated from these defects.

Since a wide spectrum of radio frequencies is monitored for PD and arcing, numerous conditions can be detected with the first test. Items that have been identified include: dirt and moisture contamination of stator windings, loose stator windings, loose lead connections, broken rotor bars, shaft currents through bearing or seal rubs, coupling misalignment, defective power supply cables, improper maintenance repairs, and defective rebuilds. An experienced test engineer is required to identify defect patterns of importance in an EMI spectrum from radio stations, data transmitters, and power electronic signals that show up at frequencies in the range of those generated by motor defects. Also, this monitoring technique does not identify the phase(s) in which stator winding PD activity is occurring.

An example of an EMI spectrum is given in Figure 13. This figure shows EMI plots for three circulating water pump motors identified as A, B, and C, with much higher μV levels for motor C. In the EMI signature for the C motor, it can be determined there is activity in the stator slots due to the high quasi-peak (QP) levels below 1,0 MHz. The QP increase near 2 MHz indicates PD activity at the core edge at the stress grading and slot coating overlap. The high QP levels at 5 MHz and higher indicates activity in the end arms. The spikes near 1 MHz are the local AM radio stations. With motors A and B, the increases of 100 kHz and 500 kHz are the local power line carriers.

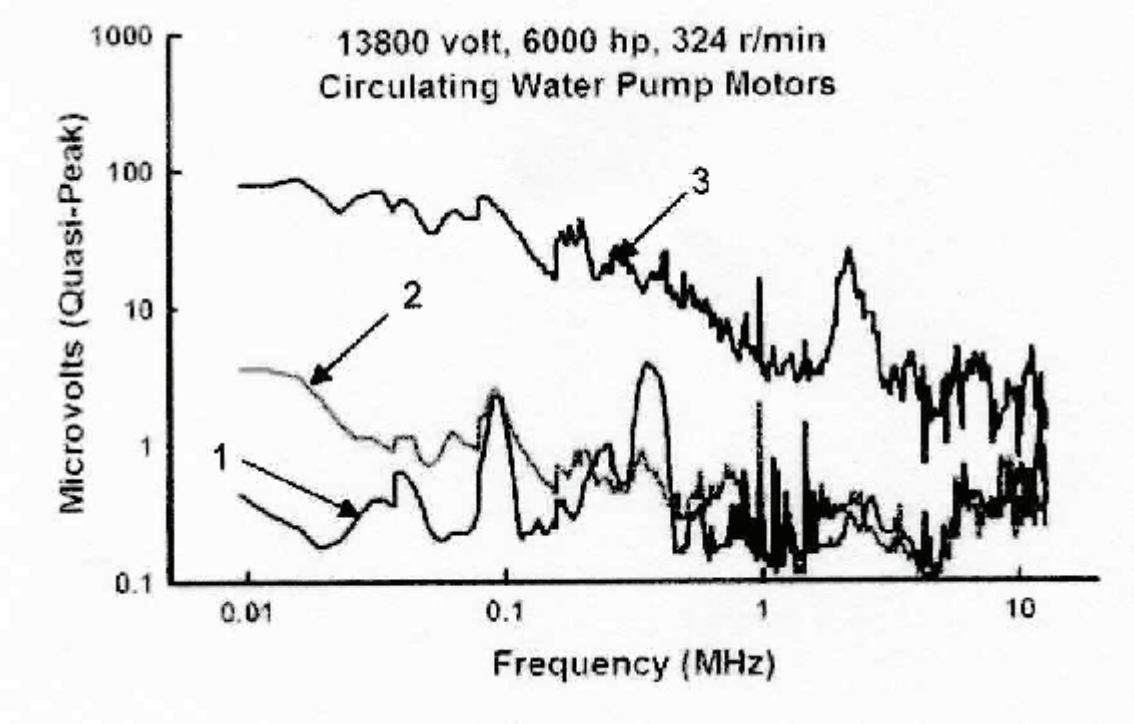

Key

1 motor A: mean = 0,4 µV 2 motor B: mean = 0,5 µV 3 motor C: mean = 14,4 µV

Figure 13 — EMI signature of motor with slot PD, voltage stress grading material deterioration, and contaminated stator endwindings

4.7 Rotor current analysis

The rotor current of an induction motor is easily accessible only in wound-rotor machines and, thus, is a less convenient monitoring parameter than the stator current. However, in such machines, the rotor circuit is poorly protected in most installations. Defects in brazed joints and slip-ring connections have often caused severe damage because they have not been detected promptly. Overheating of the rotor can also be caused by current imbalance in the external resistors connected to the slip rings.

Conventional methods of current measurement are unsatisfactory because the rotor current is at slip frequency and, thus, well below supply frequency. This low frequency demands that special air-cored current transducers, or Rogowski coils, be used instead.

4.8 Shaft voltage analysis

It is well known that any distortion in the internal flux distribution in an electrical machine can produce shaft voltages and the detrimental effects of the currents produced by such voltages have long been recognized as the cause of shaft currents that can cause bearing failures. Such shaft voltages result from asymmetry in the magnetic circuit of a motor due to variations in magnetic core steel properties within the rotating magnetic flux paths. This induces an AC voltage of the conductive loop comprising the motor shaft, the bearings, the end brackets, and the outer frame of the motor. If the induced voltage is sufficient to break down the insulation provided by the lubricant, current flows through the loop, including both bearings.

The monitoring of shaft voltages to indicate faults in the machine has not been common, as the measurements have been unreliable and inconclusive; recent developments, however, have led to some reliability and usefulness of this method.

Annex A
(informative)

Park's vector approach

As a function of the mains phase variables (i_A, i_B, i_C), the supply current Park's vector components (i_D, i_Q) are given by Formulae (A.1) and (A.2):

$$i_D = \left(\sqrt{2}/\sqrt{3}\right) i_A - \left(1/\sqrt{6}\right) i_B - \left(1/\sqrt{6}\right) i_C \quad \text{(A.1)}$$

$$i_Q = \left(1/\sqrt{2}\right) i_B - \left(1/\sqrt{2}\right) i_C \quad \text{(A.2)}$$

Under ideal conditions, balanced three-phase currents lead to a Park's vector with components as given by Formulae (A.3) and (A.4):

$$i_D = \left(\sqrt{6}/2\right) i_M \sin\left(\omega t\right) \quad \text{(A.3)}$$

$$i_Q = \left(\sqrt{6}/2\right) i_M \sin\left(\omega t - \pi/2\right) \quad \text{(A.4)}$$

where

i_M is the maximum value of the supply phase current (A);

ω is the angular supply frequency (rad/s);

t is the time variable (s).

The representation of the motor current Park's vector under healthy balanced operation is a circumference centred at the origin of the coordinate axes.

Under abnormal conditions, Formulae (A.3) and (A.4) are no longer valid and, consequently, the observed pattern is deviated according to the associated fault.

The operating philosophy of the Park's vector approach is, thus, based on identifying unique signature patterns in the loci obtained, corresponding to the supply current Park's vector representation.

Park's vector approach can be successfully used to detect a great variety of faults that can occur in three-phase induction motors. Under stator-winding fault conditions, the Park's vector pattern becomes elliptic. The ellipticity of the pattern is proportional to the fault severity and its major axis orientation depends on the faulty phase. On the other hand, the relative thickness of the ring pattern obtained, when in the presence of broken rotor slot faults in induction motors, can be utilized to diagnose such malfunctions. Under eccentricity faults in three-phase induction motors, the Park's vector pattern is recognized to have a distinctive shape. Information about the severity of the fault comes from the splitting area of the motor current Park's vector pattern.

In case of inverter-fed induction motor drives, the healthy operation pattern of the Park's vector approach is not circular; however, distinguishable deviations in the pattern can be used to diagnose faults in the power electronic components of the drive control. For example, direction of orientation of the pattern is an effective index to define any short- or open-circuit fault on one semiconductor switch.

An advanced implementation of the Park's vector approach known as the extended Park's vector approach (EPVA) is based on the spectral analysis of the AC level of the current Park's vector modulus, defined as given in Formula (A.5):

$$M = \sqrt{i_D^2 + i_Q^2} \tag{A.5}$$

The DC level, being generated mainly by the fundamental component of the motor supply current, does not contain useful information regarding the components directly related to the motor fault.

The EPVA combines the simplicity of the former Park's vector approach and the detailed insight given by the spectral analysis. Moreover, it eliminates some of the technical limitations of the conventional motor current spectral analysis. In fact, it is well known that it is sometimes difficult to filter out the fundamental component of the motor supply current without affecting the sideband components. In contrast, the characteristic components in the EPVA spectrum can easily be separated since the fundamental is far apart and its amplitude is automatically reduced by the Park's transformation. Additionally, by taking into account the current in all three phases, the EPVA provides a more meaningful spectrum than the one obtained by using the conventional motor current spectral analysis.

Being particularly useful for the diagnostics of the simultaneous occurrence of multiple machine faults, this technique produces a signature that is clear from any spectral component under healthy balanced operation and in which, under operating malfunctions, each fault is identified by the presence of specific spectral components. Broken rotor slots are identified, in the EPVA signature, by the presence of a spectral component at twice the motor slip frequency, while an eccentricity fault or mechanical load misalignment are detectable by the identification of a spectral component in the neighbourhood of the mechanical rotating frequency. A stator winding fault can be detected by the identification, in the EPVA signature, of a spectral component at twice the fundamental supply frequency.

Due to the widespread use of induction motors in industry, some of them are driving loads that are far from being constant. Compressors and time-dependent processes with low frequencies of oscillation are quite common applications. These loads introduce additional components in the motor supply currents spectrum that can mask the effects produced by an eventual rotor fault. Therefore, when in the presence of time-varying loads, the results obtained by the motor current spectral analysis can be confused with the ones obtained when the motor has a rotor fault, being almost impossible to distinguish these two working conditions.

Further developments on the use of the Park's vector approach culminate with a technique — the synchronous reference frame current Park's vector approach — that can give an indication about the rotor asymmetry, even if the motor load torque is varying in time. Under healthy balanced operation, the synchronous reference frame current Park's vector pattern [$i_Q = f(i_D)$] is a single dot. For the case of a rotor fault, it becomes an elliptic figure oriented along the second quadrant of the coordinate axes, while a time-varying load manifests itself by the appearance of an elliptic figure oriented along the first quadrant of the axes.

Bibliography

[1] ISO 13374-1, *Condition monitoring and diagnostics of machines — Data processing, communication and presentation — Part 1: General guidelines*

[2] ISO 13379 (all parts), *Condition monitoring and diagnostics of machines — Data interpretation and diagnostics techniques*

[3] ISO 13381-1, *Condition monitoring and diagnostics of machines — Prognostics — Part 1: General guidelines*

[4] ISO 17359, *Condition monitoring and diagnostics of machines — General guidelines*

[5] IEC/TS 60034-27-2, *Rotating electrical machines — Part 27-2: On-line partial discharge measurements on the stator winding insulation of rotating electrical machines*

[6] IEC 60270, *High-voltage test techniques — Partial discharge measurements*

[7] IEEE 1434, *IEEE guide to the measurement of partial discharges in rotating machinery*

[8] CISPR 16-1-1, *Specification for radio disturbance and immunity measuring apparatus and methods — Part 1-1: Radio disturbance and immunity measuring apparatus — Measuring apparatus*

[9] NEMA MG 1-2011, Revision 1-2010, Motors and generators

[10] Benbouzid M.E.H. Bibliography on induction motors faults detection and diagnosis. *IEEE Trans. Energ. Convers.* 1999, **14** pp. 1065–1074

[11] Cardoso A.J.M., Cruz S.M.A., Fonseca D.S.B. Inter-turn stator winding fault diagnosis in three-phase induction motors, by Park's vector approach. *IEEE Trans. Energ. Convers.* 1999, **14** pp. 595–598

[12] Cardoso A.J.M., & Saraiva E.S. Computer-aided detection of air-gap eccentricity in operating three-phase induction motors by Park's vector approach. *IEEE Trans. Ind. Appl.* 1993, **29** pp. 897–901

[13] Cruz S.M.A., & Cardoso A.J.M. Rotor cage fault diagnosis in three-phase induction motors by extended Park's vector approach. *Electric Machines and Power Systems.* 2000, **28** pp. 289–299

[14] Cruz S.M.A., & Cardoso A.J.M. Stator winding fault diagnosis in three-phase synchronous and asynchronous motors by the extended Park's vector approach. *IEEE Trans. Ind. Appl.* 2001, **37** pp. 1227–1233

[15] Culbert I.M., Dhirani H., Gupta B.K.On-line measurement of partial discharges on large motors in a generating station. In: *Proceedings: Electrical Insulation Conference and Electrical Manufacturing and Coil Winding Conference*, Cincinnati, OH, pp. 537–540, 2001

[16] Culbert I.M., & Rhodes W. Using current signature analysis technology to reliably detect cage winding defects in squirrel cage induction motors. *IEEE Trans. Ind. Appl.* 2007, **43** pp. 422–442

[17] Duyar A., & Bates A. Motor condition monitoring; MCM; An inexpensive, simple to use model based condition monitoring technology. *J. Maintenance Asset Management.* 2006, **21** pp. 13–22

[18] Gross D.W.Partial discharge monitoring of rotating machines — application networking and interpretation, 10th EPRI Steam Turbine-Generator Workshop, Phoenix, AZ, 2007-08

[19] Kilman G.B., & Stein J.Induction motor fault detection via passive current monitoring, Proc Int. Conference (ICEM'90), MIT, Boston, MA, 1990, pp. 13–17

[20] Schoen R.R., Habetler T.G., Kamran F., Bartfield R.G. Motor bearing damage detection using stator current monitoring. *IEEE Trans. Ind. Appl.* 1995, **31** pp. 1274–1279

[21] Stone G.C., Boulter E.A., Culbert I.M., Dhirani H. *Electrical insulation for rotating machines — Design, evaluation, aging, testing and repair*. Hoboken, NJ: Wiley–IEEE Press, 2004

[22] Stone G.C., & Warren V. Objective methods to interpret partial-discharge data in rotating-machine stator windings. *IEEE Trans. Ind. Appl.* 2006, **42** pp. 195–200

[23] Tavner P.J., & Penman J. *Condition monitoring of electrical machines*. Letchworth: Research Studies Press, 1987

[24] Thomson W.T., & Fenger M. Current signature analysis to detect induction motor faults. *IEEE Ind. Appl. Mag.* 2001, **7** (4) pp. 26–34

[25] Thomson W.T., Fenger M., Lloyd B.Development of a tool to detect faults in induction motors via current signature analysis, 2003 IEEE-IAS/PCA Cement Industry Conference, Dallas, TX, 2003-05-04/09

[26] Thomson W.T., & Gilmore R.J.Motor current signature analysis to detect faults in induction motors — Fundamentals, data interpretation and industrial case histories. In: Proceedings of the 32nd Turbomachinery Conference, 2003

[27] Thomson W.T., & Rankin D.Case histories of rotor winding fault diagnosis in induction motors. In: 2nd Int. Conf Proc on Condition Monitoring, University College Swansea, 1987-03

[28] Timperley J.E., & Chambers E.K.Locating defects in large rotating machines and associated electrical systems through EMI Diagnostics. 34th Session of CIGRE, paper 11-311, Paris, 1992-09

[29] Timperley J.E., & Michalec J.R. Reliability of operation through proper specification of rotating machinery. *IEEE Trans. Ind. Appl.* 1993, **29** pp. 225–232

[30] Timperley J.E., & Nichols D.K.Measurement of 2,300 volt motor defects with on-line EMI diagnostic techniques. In: IEEE DEIS International Symposium on Electrical Insulation, Arlington, VA, 1998-06

ICS 29.160.30;17.160
Price based on 24 pages